Stable Isotope Geochemistry: A Tribute to Samuel Epstein
© The Geochemical Society, Special Publication No. 3, 1991
Editors: H. P. Taylor, Jr., J. R. O'Neil and I. R. Kaplan

An experimental study of oxygen isotope partitioning between silica glass and CO_2 vapor

EDWARD STOLPER and SAMUEL EPSTEIN
Division of Geological and Planetary Sciences, California Institute of Technology, Pasadena, CA 91125, U.S.A.

Abstract—The fractionation of oxygen isotopes between CO_2 vapor and silica glass was determined at a total pressure of ~0.5 bars at temperatures of 550–950°C. Experiments were conducted by equilibrating a small amount of CO_2 gas with a large amount of silica glass of known isotopic composition. Because most of the oxygen in the system is in the glass, its oxygen isotope ratio changes negligibly over the course of the experiment, and the fractionation factor (α) can be determined by measurement of the isotopic composition of CO_2 in the vapor at the end of the experiment. Results are independent of the grain size of the silica glass and of time in long duration runs; these are among the criteria used to conclude that isotopic equilibrium was achieved.

The $\delta^{18}O$ value of CO_2 vapor is higher than that of coexisting silica glass at equilibrium. The fractionation factor decreases from 1.0042 ± 0.0002 at 550°C to 1.0022 ± 0.0002 at 950°C. Ln(α) is linear with $1/T$ over the temperature range we investigated, corresponding to a standard state enthalpy change for the isotopic exchange reaction of approximately −10 cal/mole. The reduced partition function ratio for silica glass is well described by multiplying that of crystalline quartz by 1.035. Comparison of our results with data in the literature on crystalline quartz suggests that silica glass is enriched in ^{18}O relative to quartz with which it is in isotopic equilibrium by 0.3–0.6 per mil over the temperature range we have investigated. This appears to confirm previous suggestions that oxygen isotopic fractionations between crystalline and amorphous materials of the same composition and similar short-range structures are small. In contrast to the CO_2-silica glass fractionation factor, the logarithm of the crystalline quartz-silica glass fractionation factor is expected to be roughly proportional to $1/T^2$ over the temperature range of this study.

Experiments were also conducted to determine the kinetics of oxygen isotopic exchange between CO_2 vapor and silica glass. The activation energy for apparent self-diffusion of oxygen in the glass is similar to those for diffusion of Ar and molecular CO_2, O_2, and H_2O in silica-rich glasses. This suggests that isotopic exchange in our experiments occurs by diffusion of CO_2 molecules into the glass followed by exchange with the oxygen atoms of the glass structure and that the rate limiting step is the diffusion of the CO_2 molecules, not their reaction with the glass network.

INTRODUCTION

FRACTIONATION FACTORS FOR oxygen isotopes provide essential constraints on interpretations of their distributions in natural systems and for understanding the principles underlying their behavior. There have been over the years many efforts to determine vapor-mineral and mineral-mineral fractionation factors (see review by O'NEIL, 1986), and recent studies suggest that in some of the most critical of these systems, workers may be converging on the correct values (*e.g.*, CLAYTON *et al.*, 1989; CHIBA *et al.*, 1989; CHACKO *et al.*, 1991). However, few measurements have been made of fractionation factors involving silicate melts or glasses, even though knowledge of such fractionation factors is necessary for understanding the behavior of oxygen isotopes during igneous processes.

Studies of oxygen isotope fractionations between coexisting crystals and naturally occurring glass (or groundmass, usually assumed to be representative of a melt phase) have shown that for some minerals, mineral-melt fractionations can be on the order of a few per mil at magmatic temperatures and that melt composition and crystal chemistry exert strong controls on fractionation factors (*e.g.*, GARLICK, 1966; TAYLOR, 1968; ANDERSON *et al.*, 1971; MATSUHISA, 1979). However, little experimental work has been done that is relevant to the fractionation of oxygen isotopes between silicate glasses or melts and other phases. MUEHLENBACHS and KUSHIRO (1974) measured oxygen isotope fractionations between 1 atm of CO_2 (or O_2) vapor and basaltic melt, plagioclase, and enstatite at 1250–1500°C. MUEHLENBACHS and SCHAEFFER (1977) estimated from these results that at 1150–1430°C, oxygen gas has about a two per mil higher $^{18}O/^{16}O$ ratio than coexisting silica glass. MATSUHISA *et al.* (1979) reported a single determination for hydrous albitic melt and water at 825°C, 3 kbar (0.0 per mil) and estimated that oxygen isotope fractionation between crystalline albite and hydrous albitic melt under these conditions may be as small as 0.2 per mil. CONNOLLY and MUEHLENBACHS (1988) state that melilite, "basalt," and "silicate glass" all have 2.33 per mil lower $^{18}O/^{16}O$ ratios than coexisting CO_2 gas.

In this paper, we report the results of experiments to determine the fractionation of oxygen isotopes

between CO_2 vapor and silica glass at 550–950°C, $P \sim 0.5$ bar. Although these results are not directly applicable to mineral-melt fractionation factors in complex igneous systems, in combination with available data on CO_2-quartz fractionations they provide data relevant to fractionations among crystalline and amorphous silicates. They also can be used to evaluate the hypothesis that oxygen isotope fractionations between minerals and melts of the same composition are small (GARLICK, 1966; MATSUHISA *et al.*, 1979) and to predict the likely dependence of mineral-melt fractionation factors on temperature.

EXPERIMENTAL TECHNIQUES

The design of our experiments was similar in principle to that employed by O'NEIL and EPSTEIN (1966) in their study of the partitioning of oxygen and carbon isotopes among calcite, dolomite, and CO_2 vapor and by LIU and EPSTEIN (1984) in their study of the partitioning of hydrogen isotopes between kaolinite and water vapor. In each experiment, a small amount of CO_2 gas (typically a few tens of micromoles) of known isotopic composition was sealed in a tube along with a large amount of silica glass (up to several grams) of known isotopic composition, and held at elevated temperature and allowed to exchange oxygen isotopes. Once equilibrium is achieved in such experiments, the fractionation factor can be determined simply by measuring the isotopic composition of the CO_2 because the oxygen isotope ratio of the silica glass (which contains most of the oxygen in the system) changes negligibly over the course of the experiment. By using fine-grained glass as the starting material, the success of the experiment does not require complete exchange between the gas and the entire silicate sample; *i.e.*, by maximizing the surface area to volume ratio of the silicate, it is possible for the number of oxygen atoms sufficiently deep within the glass so as to be representative of the bulk glass yet still near enough to the surface to be readily exchanged to far exceed the number of oxygens in the vapor phase.

In addition to such experiments designed to determine the equilibrium fractionation factor, we conducted a series of experiments in which CO_2 gas of known isotopic composition was sealed in empty silica and Vycor glass tubes and allowed to exchange for varying times in order to set constraints on the kinetics of oxygen isotope exchange between CO_2 gas and silica-rich glass.

Starting materials

Experiments were conducted on three different batches of silica glass. Most experiments were conducted on samples taken from a batch of silica glass wool (referred to as Qtz Wool 1) with an average thread diameter of about 10 μm. A smaller number of experiments was conducted on a second batch of quartz wool with a similar average thread diameter (referred to as Qtz Wool 3; manufactured by Heraeus Amersil, Inc.). The third batch of glass was prepared from chunks of General Electric #214 fused quartz (referred to as GE214) by crushing in a stainless steel mortar followed by dry sieving with nylon screens. Most experiments on this material were conducted on a <400 mesh (<37 μm) fraction, but several experiments were conducted on 325–400 mesh (37–44 μm) and 200–325 (44–74 μm) size fractions. The $\delta^{18}O_{SMOW}$ values of the three batches of glass are +14.1 (Qtz Wool 1), +16.8 (Qtz Wool 3), and +11.2 (GE214). Techniques for isotopic analysis of these glasses and precision of the analyses are discussed below.

One of three sources of CO_2 gas was used in each experiment: a tank of liquid CO_2 ($\delta^{18}O_{SMOW} \approx -1$); CO_2 prepared from commercial $CaCO_3$ powder ($\delta^{18}O_{SMOW} \approx +20$); or CO_2 prepared from a conch shell (Strombus gigas; $\delta^{18}O_{SMOW} \approx +42$). Techniques for isotopic analysis of the gases and precision of the analyses are discussed below.

Experiments

Silica glass wool or powder (0.3–2.2 g) was placed in a fused quartz (General Electric #214; $\delta^{18}O_{SMOW} = +11.2$; <5 ppm by weight OH^-) or Vycor glass (Corning Code No. 7913; 96% SiO_2; $\delta^{18}O_{SMOW} = +20.7$) tube with an OD of 9 mm and an ID of 7 mm. Tubes were typically ~15 cm long. After heating in air for 20–30 minutes at 850°C to oxidize any organic contaminants in the samples and tubes, the loaded tubes were attached to a vacuum line and 30–75 μmoles of CO_2 were frozen into the tube along with the glass sample, after which the tube was sealed with a torch. Tubes were loaded into the hotspots of home-built, wire-wound horizontal furnaces and held at 550, 650, 750, 850, or 950°C (monitored with Type K or S thermocouples located at the hotspot) for 1–428 days. Hotspot temperatures were controlled by Eurotherm temperature controllers (model 808) and typically varied by less than 1°C. Temperature gradients were such that the temperature varied by at most 15°C over the length of each sample tube, and typically less than 5°C over the segment of the tube containing the silica glass sample. Many experiments could be run simultaneously in each furnace; transient temperature fluctuations up to several tens of degrees and lasting several minutes were experienced when cold samples were introduced into an already hot furnace. For several experiments, samples were first held at one temperature for sufficient time (based on other experiments) to closely approach equilibrium, then placed in a furnace at a higher or lower temperature and allowed to approach equilibrium at the second temperature. For a few experiments, the run products and/or tubes from previous experiments were reused in later experiments, and in others about 0.6 μmoles of H_2O was loaded into the tube along with the sample and the CO_2.

Analysis of Qtz Wool 1 material after a 850°C, 30 minute preheating in air gave a value within 1σ of the mean value (see below), indicating that our procedure for removing organics does not significantly influence the bulk isotopic composition of the starting material, although some exchange between oxygen near the surfaces of the threads and air undoubtedly occurred. Based on our determination of the self-diffusion coefficient for oxygen in silica glass (see below), the depth of penetration of oxygen exchange during the preheating would be about 0.03 μm.

Several experiments were conducted by sealing 37–132 μmoles of the CO_2 prepared from the conch shell inside GE214 fused quartz or Vycor glass tubes (preheated at 850°C in air for 30 minutes) without any silicate sample, and then holding these tubes at 550–850°C for 1 hour to 153 days to examine the kinetics of exchange between the glass tube and CO_2.

Analytical techniques

After removal from the furnace and cooling in air, each tube was cracked on an extraction line; the CO_2 was col-

lected, its quantity measured manometrically, and its $\delta^{18}O$ and $\delta^{13}C$ analyzed on a mass spectrometer. Starting materials and several run products were examined by scanning electron microscopy; no changes were detected. X-ray diffraction measurements on run products showed no evidence of crystallization of the glasses over the course of the experiments.

To evaluate the precision of our mass spectrometric analyses of CO_2, we prepared a large batch of CO_2 from the conch shell and sealed ~100–150 μmoles into each of about 50 pyrex tubes. The gas from one or more of these tubes was analyzed in most of the sessions on the mass spectrometer during which the gases extracted from our experiments were analyzed. Based on 13 such analyses obtained over more than a year, the precision of the $\delta^{18}O$ values we report for CO_2 gas is 0.14 per mil (1σ).

Oxygen was extracted from the starting materials by reaction with either BrF_5 or F_2 and then reacted with graphite to produce CO_2 that was then analyzed mass spectrometrically. Precisions of the isotopic analyses of the starting materials include contributions both from uncertainties in the mass spectrometry and from uncertainties introduced during the extraction procedure. Multiple analyses of the starting materials suggest a procedural contribution to the uncertainty in our silicate $\delta^{18}O$ values of about 0.1 per mil (1σ). Accuracy of the oxygen isotope analyses is difficult to assess and, except for systematic inaccuracies introduced during the extraction procedure, is of little consequence to us since we are primarily interested in differences between measurements. However, Professor R. Clayton and T. Mayeda of the University of Chicago analyzed samples of the Qtz Wool 1 and GE214 glass for us and obtained $\delta^{18}O_{SMOW}$ values of +13.8 and +10.9 compared to our values of +14.1 and +11.2. Previous comparisons have also shown that $\delta^{18}O$ values obtained at Caltech are characteristically higher than those reported by the Chicago group by about 0.3 per mil (H. P. TAYLOR, pers. comm.).

RESULTS

Silica glass exchange experiments.

Results of all experiments on silica glass are listed in Tables 1–3 and representative results on Qtz Wool 1 and GE214 are shown graphically versus run duration in Figs. 1 and 2. Our best estimates of the fractionation factors for each sample at each temperature are listed in Table 4 and shown versus $10^6/T\,(K)^2$ in Fig. 3. At each temperature, the fractionation factors determined for the three starting materials are essentially identical. For the quartz wool samples at 550–850°C, these values are averages of all results obtained at durations long enough so that results similar within error were obtained. For the quartz wool samples at 950°C, only samples run in silica glass tubes were included in the averages, although for the Qtz Wool 3 experiments, when samples and tubes were reused from previous experiments, results were similar whether silica or Vycor tubes were used. For the GE214 experiments, only the results of experiments on the <37 μm size fraction were included in the averages, and then only if the run duration was sufficiently long that the results appeared independent of run duration.

In the context of our study, a "reversal" is a pair of experiments in which the $\delta^{18}O$ of the gases from two experiments run at the same temperature approached the equilibrium value from a starting value heavier than the equilibrium value in one experiment and from a value lighter than the equilibrium value in the other. Reversals are available over most of the temperature range for all three starting materials. In some experiments, the direction from which the equilibrium gas composition was approached was controlled by pre-equilibrating the gas and the silica glass rather than by loading a starting gas with a particular $\delta^{18}O$ value. For example, experiment #15B (Table 1) was first equilibrated with glass wool for 31 days at 650°C, during which time the $\delta^{18}O_{SMOW}$ of the gas *decreased* from the starting value of +20 to a value of +18.0 (based on the results of #15C, run simultaneously under identical conditions); after removal from the 650°C furnace, the sealed tube was then placed in the 550°C furnace for 76 days, during which time the $\delta^{18}O_{SMOW}$ of the CO_2 gas *increased* to a final value of +18.7. Four experiments of this sort were conducted, giving values at 550, 650, 750, and 850°C. In every case, including runs such as #15C in which the final $\delta^{18}O$ value was overshot in the pre-equilibration stage, the results of these experiments were indistinguishable from the values we report as the equilibrium values based only on long duration runs held only at a single temperature.

Long duration runs on the 37–44 μm size fraction of the GE214 starting material at temperatures $\geq$ 650°C yield results indistinguishable from reversed results of shorter experiments conducted on the <37 μm size fraction (Fig. 2). Lengthy experiments on this size fraction at 550°C approach to within 0.4 per mil of the results on finer size fractions at shorter times. Similarly, reversal experiments on the 44–74 μm size fraction reproduce results on finer size fractions in experiments of sufficiently long duration (*e.g.*, runs #23R and #23V at 850°C; Fig. 2). Results at the lower temperatures on the 37–44 μm size fraction are in most cases also consistent with the results on finer grained samples, but some experiments appear to have incompletely exchanged (*e.g.*, runs #23S and #23T at 550 and 650°C). All experiments at 950°C on the GE214 starting material yield gas anomalously rich in ^{18}O; this could reflect a transient because all of these experiments were of short duration, or perhaps incipient crystallization of the glass, although X-ray and optical evidence do not support this latter suggestion.

Table 1. Qtz wool 1 experimental conditions and results

Sample[a]	T (°C)[b]	Duration (days)[b]	Tube[c]	μmoles CO_2 (initial)[d]	Yield (%)[d]	$\delta^{13}C_{PDB}$ (‰, initial)	$\delta^{13}C_{PDB}$ (‰, final)	$\delta^{18}O_{SMOW}$ (‰, initial)	$\delta^{18}O_{SMOW}$ (‰, final)	wt (g)[e]	SiO_2/CO_2[f]
#6B	550	71.9	q	57.3	101.0	−13.0	−13.0	20.0	17.7	0.61	176
#6D	550	12.9	q	50.9	105.1	−30.1	−30.0	0.0	16.2	0.59	192
#6F	550	30.2	q	47.7	107.8	−0.4	−0.6	41.9	18.7	0.55	191
#15B	650/550	30.8/76.2	q	44.4	97.5	−12.9	−12.8	20.1	18.7	1.03	386
#15E	550	94.8	q	42.3	99.1	−30.1	−29.8	0.0	18.2	0.99	390
#15I	550	91.0	q	40.1	99.3	−12.8	−12.9	19.8	18.7	1.02	422
#16A	550	66.8	v	37.3	98.7	−12.9	−13.0	20.1	18.5	1.03	460
#16G	550	152.8	v	40.0	96.5	−12.9	−12.6	20.1	18.7	0.92	383
#22B	550	231.9	v	39.8	103.3	−12.8	−12.9	20.1	18.5	0.96	400
				35.4					18.6		
#22D	550	231.9	q		98.6	−12.8	−12.8	20.1	18.2	1.04	488
							−12.9		18.1		
									18.0		
									18.0		
#6A	650	12.9	q	65.3	102.8	−13.0	−13.0	20.0	17.1	0.52	133
#6C	650	12.9	q	58.8	102.7	−30.1	−29.9	0.0	16.9	0.66	187
#6E	650	10.9	q	47.7	109.6	−0.4	−0.5	41.9	17.9	0.59	206
#15C	650	30.8	q	45.3	102.2	−12.9	−12.8	20.1	18.1	1.02	375
			q				−12.8		18.1		
#15G	750/650	30.8/29.0	q	44.5	98.2	−30.1	−30.0	0.0	18.0	1.01	378
#15K	650	43.8	q	46.3	97.8	−29.8	−29.5	−0.2	18.1	0.98	352
#16E	650	30.8	v	44.4	105.9	−12.9	−12.9	20.1	18.0	1.01	379
#16F	650	66.7	v	43.1	97.2	−12.9	−12.9	20.1	17.9	0.97	375
#22A	650	231.9	v	35.4	99.7	−12.8	−12.8	20.1	17.5	1.06	497
									17.6		
							−12.8		17.6		
									17.5		
#22C	650	231.9	q	35.4	96.0	−12.8	−12.8	20.1	18.5	1.04	488
									18.0		
									18.0		
#22E	650	2.0	q	52.0	96.9	−12.8	−12.8	20.1	17.8	0.52	167
#22F	650	4.7	q	52.0	100.2	−12.8	−12.8	20.1	17.5	0.49	158
#22G	650	6.7	q	51.9	96.9	−12.8	−12.9	20.1	17.6	0.55	176
#22H	650	8.7	q	51.9	99.4	−12.8	−12.8	20.1	17.9	0.49	159
#22I	650	10.9	q	51.5	99.6	−12.8	−12.8	20.1	17.9	0.50	162
#22J	650	15.7	q	51.1	100.4	−12.8	−12.8	20.1	17.9	0.50	161
#22K	650	20.9	q	51.1	100.4	−12.8	−12.9	20.1	18.0	0.50	164
#22L	650	30.0	q	50.2	100.4	−12.8	−12.7	20.1	17.8	0.49	163
#22M	650	66.7	q	50.2	98.6	−12.8	−12.8	20.1	17.8	0.53	176
#22N	650	120.9	q	50.2	96.8	−12.8	−12.6	20.1	17.9	0.49	162
#3C[g]	750	12.1	q	55.0	102.2	−0.5	−0.6	42.2	17.1	0.53	160
#3D[g]	750	12.1	q	29.0	92.1	−0.5	−1.2	42.2	17.2	0.69	393
#3E[g]	750	12.1	v	25.9	106.2	−0.5	−1.2	42.2	17.3	0.55	355

Table 1. (Continued)

Sample[a]	T (°C)[b]	Duration (days)[b]	Tube[c]	μmoles CO_2 (initial)[d]	Yield (%)[d]	$\delta^{13}C_{PDB}$ (‰, initial)	$\delta^{13}C_{PDB}$ (‰, final)	$\delta^{18}O_{SMOW}$ (‰, initial)	$\delta^{18}O_{SMOW}$ (‰, final)	wt (g)[e]	SiO_2/CO_2[f]
#4C	750	10.8	q	44.9	104.7	−0.3	−0.4	41.8	17.7	0.65	241
#4D	750	12.1	q	40.2	101.2	−30.1	−29.9	−2.3	17.5	0.73	302
#4E	750	22.8	q	33.9	100.0	−30.1	−29.8	−2.3	17.4	0.52	255
#4F	750	25.8	q	75.3	102.8	−0.3	−0.5	41.8	17.7	0.32	71
#4H	750	22.8	q	30.7	99.0	−0.3	−1.1	41.8	17.8	0.86	466
#15D	650/750	30.8/29.0	q	47.1	98.5	−12.9	−12.9	20.1	17.1	1.07	378
#15F	750	30.8	q	47.0	98.3	−30.1	−30.0	0.0	16.9	0.94	333
#15J	750	43.8	q	41.9	99.8	−12.8	−13.0	19.8	17.7	1.02	406
#16B	750	30.8	v	50.6	101.8	−12.9	−12.7	20.1	17.2	0.99	326
#16C	750	66.8	v	48.8	104.1	−12.9	−13.6	20.1	17.3	1.02	348
#3A	850	9.0	q	40.0	120.3	−0.5	−0.9	42.2	16.6	0.62	258
#3B	850	9.0	q	21.2	108.0	−0.5	−0.5	42.2	16.6	0.37	287
#3F	850	9.0	v	32.2	103.1	−0.5	−0.6	42.2	16.7	0.47	243
#4A	850	8.9	q	41.8	104.3	−0.3	−0.4	41.8	17.4	0.77	307
#4B	850	38.9	q	44.9	102.4	−0.3	−0.5	41.8	17.2	0.56	208
#4G	850	10.2	q	37.0	100.5	−30.1	−29.8	−2.3	16.6	0.65	292
#4I	850	20.8	q	48.1	101.0	−0.3	−0.4	41.8	17.1	0.73	253
#4J	850	20.8	q	33.9	102.4	−30.1	−29.8	−2.3	16.8	0.81	398
#15A	850	30.8	q	42.6	98.4	−12.9	−12.7	20.1	16.9	0.76	297
							−12.8		17.0		
#15H	750/850	30.8/29.0	q	47.9	96.5	−30.1	−29.9	0.0	16.8	1.05	365
#16D	850	30.8	v	45.7	104.6	−12.9	−12.8	20.1	17.2	0.89	324
#16H	850	66.8	v	40.9	98.0	−12.9	−12.9	20.1	16.7	0.95	387
#20A	950	8.0	q	64.8	96.9	−29.9	−29.8	−0.5	16.6	0.99	254
#20I	950	8.0	q	65.6	98.2	−13.0	−13.0	20.0	16.3	1.12	283
#25C	950	67.0	qr(20A)	42.5	100.2	−30.0		−0.3	16.0	0.99	387
#25M	950	67.0	qr(20I)	40.6	102.7	−12.6	−12.9	20.6	16.2	1.12	457
#20E	950	8.0	v	63.9	100.9	−29.9	−30.1	−0.5	17.0	1.02	267
#20M	950	8.0	v	64.7	99.5	−13.0	−12.9	20.0	17.0	1.01	260
#25H	950	67.0	vr(20E)	41.6	101.4	−30.0		−0.3	17.1	1.02	410
#25R	950	67.0	vr(20M)	39.3	101.8	−12.6		20.6	17.0	1.01	429

Notes for Tables 1–3:

[a] Sample numbers in italics indicate runs the results of which were included in the averages listed in Table 4. Unlabeled rows correspond to repeat analyses of the gas extracted from the sample indicated by the last labelled row above.

[b] Samples that were first held at one temperature for a given duration and then transferred to a second temperature for a second duration are indicated in these columns as x/y, where x is the initial temperature or run duration and y is the second temperature or run duration.

[c] v = Vycor tube; q = GE214 quartz glass tube. qr and vr indicate experiments in which the silicate sample and the quartz glass and Vycor tubes from a previous experiment were reused with a fresh aliquot of CO_2; the number in parentheses corresponds to the experiment in which the tube and sample were previously used. When a number is given in parentheses but there is no "r" designation, it signifies that the sample from the experiment indicated in parentheses was reloaded along with a new batch of CO_2 into a new tube and rerun.

[d] Measured number of micromoles of CO_2 loaded into the capsule at the start of the experiment and the measured yield of CO_2 extracted at the close of the experiment in percent of the initial, as loaded, value.

[e] Mass of silica glass loaded into the capsule.

[f] Ratio of moles of silica glass to CO_2 loaded into the capsule.

[g] Samples contain ~0.6 micromoles of H_2O in addition to CO_2.

[h] Grain size based on nominal sizes of nylon sieves used to divide the sample into size fractions. The size fraction that passed through a 400 mesh sieve is designated <37 μm.

Table 2. Qtz wool 3 experimental conditions and results

Sample[a]	T (°C)	Duration (days)	Tube[c]	μmoles CO_2 (initial)[d]	Yield (%)[d]	$\delta^{13}C_{PDB}$ (‰, initial)	$\delta^{13}C_{PDB}$ (‰, final)	$\delta^{18}O_{SMOW}$ (‰, initial)	$\delta^{18}O_{SMOW}$ (‰, final)	wt (g)[e]	SiO_2/CO_2[f]
#25A	750	66.2	qr (24A)	40.7	100.7	−30.0	−30.0	−0.3	19.5	1.38	563
#25F	750	66.2	vr (24D)	42.5	98.1	−30.0		−0.3	20.1	1.74	683
#25K	750	66.2	qr (24G)	37.9	105.5	−12.6		20.6	19.5	1.23	542
#25P	750	66.2	vr (24J)	39.9	100.3	−12.6		20.6	19.6	1.68	701
#25D	750	66.2	q	41.7	103.1	−30.0		−0.3	19.9	1.52	605
#25J	750	66.2	v	41.3	101.0	−30.0		−0.3	20.1	1.96	788
#25N	750	66.2	q	40.7	102.5	−12.6		20.6	20.4	2.09	855
#25S	750	66.2	v	39.1	102.6	−12.6		20.6	21.1	2.05	874
#24A	950	84.0	q	41.9	99.5	−30.1	−29.8	−0.4	19.0	1.38	547
#24B	950	32.8	q	41.0	102.4	−30.1	−29.8	−0.4	20.1	1.74	707
#24C	950	66.3	q	42.3	100.5	−30.1	−29.9	−0.4	19.6	1.63	640
#24D	950	84.0	v	42.3	98.6	−30.1	−29.7	−0.4	19.2	1.74	686
#24E	950	32.8	v	41.4	102.7	−30.1	−29.9	−0.4	19.9	1.16	466
#24F	950	66.3	v	42.3	101.2	−30.1	−30.0	−0.4	21.4	1.71	672
#24G	950	84.0	q	43.2	98.4	−12.9	−12.9	20.1	19.2	1.23	476
#24H	950	32.8	q	43.2	100.5	−12.9	−13.2	20.1	19.6	1.28	494
#24I	950	66.3	q	43.2	102.5	−12.9	−13.3	20.1	19.3 19.4	1.46	564
#24J	950	84.0	v	43.2	101.6	−12.9	−13.6	20.1	19.2	1.68	648
#24K	950	32.8	v	42.4	106.4	−12.9	−13.3	20.1	21.2	1.72	677
#24L	950	66.3	v	41.5	105.3	−12.9	−13.4	20.1	21.3	1.82	729
#25E	950	67.0	q	41.7	104.3	−30.0		−0.3	18.9	1.96	782
#25I	950	67.0	v	41.6	101.4	−30.0		−0.3	19.3	2.06	823
#25O	950	67.0	q	40.6	103.0	−12.6		20.6	19.7	1.99	814
#25G	950	67.0	vr (24E)	42.5	102.4	−30.0		−0.3	18.8 18.7	1.16	454
#25L	950	67.0	qr (24L)	41.1	101.5	−12.6		20.6	18.9 18.9	1.28	519
#25B	950	67.0	qr (24B)	41.7	102.4	−30.0		−0.3	18.9	1.74	695
#25Q	950	67.0	vr (24K)	39.6	101.0	−12.6		20.6	19.0	1.72	725

Notes: See Table 1.

Table 3. GE214 glass powder experimental conditions and results

Sample[a]	T (°C)	Duration (days)	Tube[c]	μmoles CO_2 (initial)[d]	Yield (%)[d]	$\delta^{13}C_{PDB}$ (‰, initial)	$\delta^{13}C_{PDB}$ (‰, final)	$\delta^{18}O_{SMOW}$ (‰, initial)	$\delta^{18}O_{SMOW}$ (‰, final)	Size fraction (μm)[h]	wt (g)[e]	Silicate/CO_2[f]
#17D	550	152.8	q	38.9	102.8	−12.9	−12.5	20.1	15.8	<37	1.00	429
#18D	550	428.0	v	38.9	100.0	−12.9	−12.7	20.1	15.2	37–44	1.00	430
									15.0			
#18H	550	152.8	v	43.5	103.9	−12.9	−12.8	20.1	15.4	<37	1.01	385
#23S	550	231.9	q	42.6	93.0	−27.5	−29.0	−1.8	14.6	44–74	1.01	393
#7A	650	2.3	q	46.5	106.9	−12.9	−13.3	20.0	14.8	<37	1.83	656
#7D	650	2.3	q	46.4	104.3	−0.4	−1.0	42.0	14.8	<37	1.89	679
#17C	650	113.9	q	40.3	103.0	−12.9	−12.6	20.1	15.1	<37	1.01	417
#17G	650	113.9	q	49.9	99.0	−30.1	−29.5	0.0	15.0	<37	1.01	336
#18C	650	427.9	v	41.9	97.9	−12.9	−11.8	20.1	15.1	37–44	1.00	398
							−12.0		15.0			
							−12.0		15.0			
							−12.4		15.4			
#18G	650	113.9	v	41.9	103.3	−12.9	−12.5	20.1	15.0	<37	1.00	398
#23P	650	231.9	q	46.8	87.6	−12.7	−11.3	20.1	14.9	44–74	1.01	358
#23T	650	231.9	q	44.3	90.5	−27.5	−29.0	−1.8	14.4	44–74	1.01	378
									14.4			
									14.5			
#7B	750	1.3	q	40.1	100.0	−12.9	−12.9	20.0	15.5	<37	2.23	924
#7E	750	1.3	q	44.9	93.1	−0.4	−0.6	42.0	15.3	<37	1.68	624
#17B	750	66.8	q	43.5	96.6	−12.9	−12.4	20.1	14.5	<37	1.01	386
#17F	750	66.8	q	49.8	98.2	−30.1	−29.5	0.0	14.4	<37	1.00	335
#18B	750	114.0	v	45.1	100.0	−12.9	−12.9	20.1	14.8	37–44	1.00	370
#18F	750	66.8	v	40.3	99.5	−12.9	−12.8	20.1	14.6	<37	1.00	414
#23Q	750	231.9	q	45.0	97.8	−12.7	−12.7	20.1	15.4	44–74	1.01	372
#23U	750	231.9	q	43.4	87.8	−27.5	−28.5	−1.8	14.3	44–74	1.00	385
#7C	850	2.3	q	35.4	93.2	−12.9	−12.4	20.0	16.0	<37	2.01	944
#17A	850	30.8	q	46.6	91.6	−12.9	−12.1	20.1	14.1	<37	1.00	358
#17E	850	30.8	q	38.9	96.1	−30.1	−29.1	0.0	14.2	<37	1.00	429
#18A	850	110.8	v	48.3	104.6	−12.9	−13.0	20.1	14.1	37–44	1.00	345
#18E	850	30.8	v	43.5	102.1	−12.9	−12.7	20.1	14.2	<37	1.00	383
#23R	850	232.1	q	45.0	85.1	−12.7	−11.6	20.1	14.1	44–74	1.01	373
#23V	850	232.1	q	44.3	81.9	−27.5	−28.5	−1.8	14.0	44–74	1.01	378
#20B	950	8.0	q	65.6	83.5	−29.9	−29.0	−0.5	14.5	<37	1.00	254
#20F	950	8.0	v (7A)	65.7	93.9	−29.9	−29.7	−0.5	14.2	<37	1.04	263
#20J	950	8.0	q	63.8	88.7	−13.0	−12.0	20.0	14.9	<37	1.00	261
#20N	950	8.0	v (7B)	61.9	95.6	−13.0	−12.8	20.0	14.4	<37	1.12	300

Notes: See Table 1.

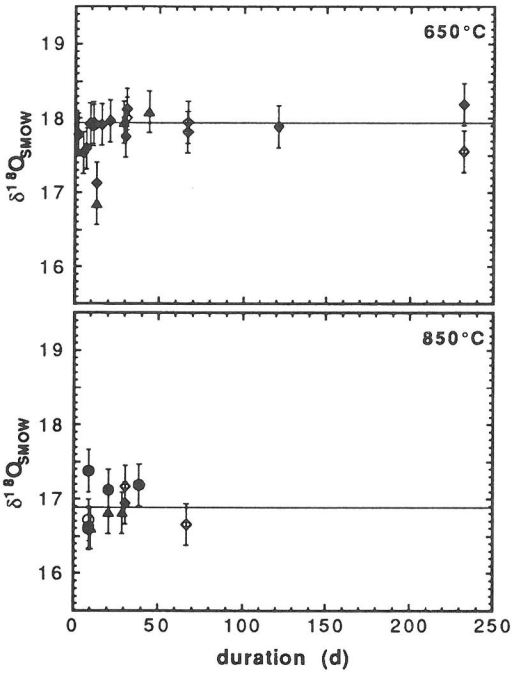

FIG. 1. Summary of CO_2 $\delta^{18}O_{SMOW}$ values for Qtz Wool 1 silica glass experiments as a function of run duration at 650 and 850°C. Error bars are $\pm 2\sigma$ for our gas analyses on our mass spectrometer (see text). Horizontal lines are averages of long duration runs (listed in Table 1 in italics); these average values are listed in Table 4 and are the values used in determining fractionation factors. Open symbols indicate experiments conducted in Vycor tubes; closed symbols indicate experiments conducted in GE214 silica glass tubes. Circles indicate experiments with a starting $\delta^{18}O_{SMOW}$ value for the CO_2 of +42; diamonds indicate a starting $\delta^{18}O_{SMOW}$ value for the CO_2 of +20; triangles indicate a starting $\delta^{18}O_{SMOW}$ value for the CO_2 of ≈ 0.

At 550 and 650°C, short duration runs (<30 days at 650°C; 70 days at 550°C) give erratic results; these may be influenced by surface fractionations (and the effects on the surfaces of the preheating step in air at 850°C) or kinetic isotope effects (see below), but results of longer experiments at these temperatures are not correlated with run duration provided runs on the same silicate size fractions are compared. Similarly, except for a few 1–2 day experiments on the GE214 powder at 750 and 850°C, results at these temperatures are not correlated with run duration over the range of run durations examined.

It is well known that water pressure enhances the apparent self-diffusion of oxygen in silica glass (PFEFFER and OHRING, 1982) and in silicate minerals and glasses generally (see review in ZHANG *et al.*, 1991b). Thus, a few experiments in which the vapor phase contained a small amount (~0.6 μmoles) of H_2O in addition to CO_2 were conducted on the Qtz Wool 1 starting material at 750°C. The final $\delta^{18}O$ values of CO_2 in the experiments that had both water and CO_2 turned out to be indistinguishable from those of samples run for comparable times but with CO_2 alone, and from experiments run with CO_2 alone but for much longer durations. This offers strong support for our conclusion that the long duration runs closely approached equilibrium.

CO_2 yields (*i.e.*, a comparison of the amount of gas initially loaded with the amount collected at the end of the experiment) are nearly all 100 ± 5% (Tables 1–3). The only significant exceptions are some of the experiments on GE214, which have yields as low as 82%. We think this is due to formation of CO by reaction of CO_2 with the minor amounts of stainless steel that contaminated this sample during crushing. This is consistent with the larger amounts (up to a few μmoles) of non-condensable (at liquid nitrogen temperatures) gas we detected in these experiments. Nevertheless, the final $\delta^{18}O$ values of CO_2 in these experiments are indistinguishable from those of experiments with yields near 100%. We

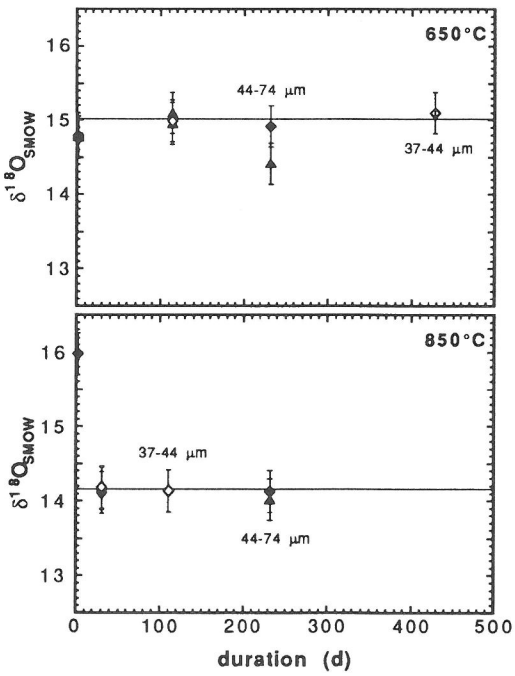

FIG. 2. Summary of CO_2 gas $\delta^{18}O_{SMOW}$ values for GE214 silica glass experiments as a function of run duration at 650 and 850°C. Error bars are $\pm 2\sigma$ for our gas analyses on our mass spectrometer (see text). Horizontal lines are averages of long duration runs (listed in Table 3 in italics) on <37 μm powder; these average values are listed in Table 4 and are the values used in determining fractionation factors. Symbols as in Fig. 1.

note that except for these samples, the concentration of non-condensable gaseous species was negligible. We often checked for water in the gas collected at the close of the experiments, and this was also usually negligible.

Results of similar experiments in silica and Vycor glass tubes at all temperatures below 950°C are usually nearly indistinguishable. The fact that there are no systematic differences between these experiments (despite the fact that the Vycor tubes are about 10 per mil heavier than the GE214 silica tubes and have self-diffusion coefficients $\approx$ 2 orders of magnitude higher; see Table 5) demonstrates that interaction of the vapor with the container does not have a significant influence on the results. However, at 950°C, results of experiments in Vycor tubes are erratic, with $\delta^{18}O$ values often much higher than expected based on lower temperature experiments run in Vycor tubes and on results of experiments run simultaneously in silica tubes. We take this as indicating that the results in Vycor at temperatures above 850°C are not reliable, probably due to extensive interaction between the CO_2 and the Vycor tube at these temperatures.

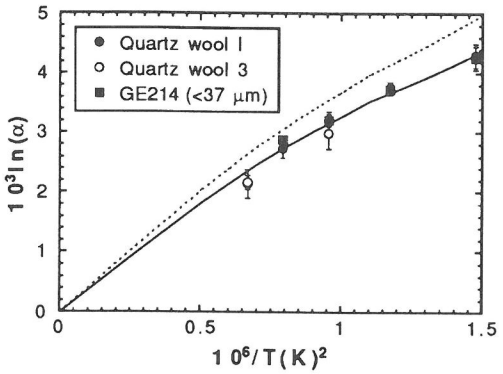

FIG. 3. Summary of CO_2-silica glass fractionation factors from this study. Errors are ±two standard errors on the equilibrium gas compositions and do not include uncertainties in the silicate analyses (see Table 4). The solid curve is calculated based on the reduced partition function ratios given for CO_2 in CHACKO *et al.* (1991) and 1.035 times the crystalline quartz-1 reduced partition function ratio given by CLAYTON *et al.* (1989). The dashed curve is the calculated CO_2-crystalline quartz fractionation factor based on these reduced partition function ratios.

In short duration experiments and at low temperatures, there is evidence for complexity in the exchange process, as anticipated by WILLIAMS (1965) and MUEHLENBACHS and SCHAEFFER (1977). For example, gas exposed to the <37 μm size fraction of the GE214 glass in runs of 1–2 days duration at 650–850°C experienced anomalous amounts of exchange and in some cases even converged from initially heavy and light $\delta^{18}O$ values to spurious, short-term "reversed" values. These observations could be evidence of surface-correlated fractionations (perhaps influenced by the 850°C preheating step) and/or kinetic isotope effects (*e.g.*, such as would be observed if there were several distinguishable oxygen sites in the glass with different fractionation factors and with different exchange rates). Similarly, in short duration experiments at 550 and 650°C on Qtz Wool 1 with starting gas heavier than the equilibrium value (based on long duration runs), the final gas is frequently lighter than the equilibrium value (see Fig. 1); *i.e.*, they appear to "overshoot" the equilibrium value. With

Table 4. Summary of experimental results on CO_2-silica glass fractionation

Sample	T (°C)	$\delta^{18}O_{SMOW}$ (‰) (final gas)	$\delta^{18}O_{SMOW}$ (‰) (silicate)	1000 ln (α) (vapor/glass)
Qtz Wool 1	550	18.49 (0.20)[a]	14.12 (0.06)[a]	4.30 (0.21)[b]
	650	17.94 (0.10)		3.76 (0.12)
	750	17.37 (0.16)		3.20 (0.17)
	850	16.89 (0.16)		2.73 (0.17)
	950	16.29 (0.24)		2.14 (0.25)
Qtz Wool 3	750	19.86 (0.26)	16.82 (0.16)	2.99 (0.30)
	950	19.02 (0.12)		2.16 (0.20)
GE214	550	15.56 (0.20)	11.24 (0.11)	4.26 (0.23)
	650	15.02 (0.09)		3.73 (0.14)
	750	14.49 (0.09)		3.21 (0.14)
	850	14.16 (0.05)		2.88 (0.12)

[a] Numbers in parentheses are 2σ of the mean of the analyses used to compute the average of gas analyses from all successful experiments or silicate extractions, except for GE214 at 550°C where there were only two successful experiments. The reported error in this case is one-half of the difference in $\delta^{18}O$ between the two results.

[b] Numbers in parentheses are 2σ errors based on propagation of the errors on the gas and silicate analyses reported in the two previous columns.

Table 5. Diffusion experiments: experimental conditions and results

Sample	T (°C)	Duration (days)	Tube[a]	μmoles CO_2 (initial)[b]	Yield (%)[b]	$\delta^{13}C_{PDB}$ (‰, initial)	$\delta^{13}C_{PDB}$ (‰, final)	$\delta^{18}O_{SMOW}$ (‰, initial)	$\delta^{18}O_{SMOW}$ (‰, final)	Tube length (cm)[c]	$\log_{10}(D)$ (cm^2/s)[d]
#10O	550	0.2	q	44.8	95.1	−0.5	−0.5	41.8	40.0	15.7	−15.5 (0.2)
#12K	550	2.0	q	56.7	96.8	−0.4	−0.4	42.0	39.6	14.6	−16.0 (0.2)
#12C	550	4.0	q	45.3	100.4	−0.4	−0.4	42.0	37.8	16.6	−16.1 (0.1)
#12D	550	8.0	q	45.3	98.5	−0.4	−0.4	42.0	37.1	15.2	−16.2 (0.1)
#12E	550	16.0	q	44.4	100.5	−0.4	−0.5	42.0	34.5	16.3	−16.1 (0.1)
#12A	550	32.0	q	61.1	100.3	−0.4	−0.4	42.0	34.8	16.3	−16.1 (0.1)
#12B	550	64.0	q	62.0	97.6	−0.4	−0.6	42.0	34.9	16.8	−16.5 (0.1)
#14F	550	66.8	q	173.4	96.7	−1.2	−1.1	40.5	36.4	15.4	−16.1 (0.1)
#14G	550	152.8	q	163.5	97.4	−1.2	−1.0	40.5	35.3	14.3	−16.1 (0.1)
#12L	650	1.0	q	41.9	97.6	−0.4	−0.5	42.0	37.3	15.2	−15.4 (0.1)
#12J	650	2.0	q	40.9	98.0	−0.4	−0.4	42.0	36.5	15.6	−15.6 (0.1)
#12I	650	4.0	q	40.9	100.0	−0.4	−0.7	42.0	35.2	15.7	−15.6 (0.1)
#12F	650	8.0	q	44.4	96.4	−0.4	−0.4	42.0	33.4	16.7	−15.7 (0.1)
#12H	650	16.0	q	40.9	95.6	−0.4	−0.4	42.0	34.2	16.4	−16.1 (0.1)
#12G	650	32.0	q	39.2	95.7	−0.4	−0.3	42.0	30.4	17.2	−16.0 (0.1)
#14D	650	66.8	q	180.3	99.8	−1.2	−1.2	40.5	34.0	15.3	−15.5 (0.1)
#14E	650	152.8	q	177.4	99.2	−1.2	−1.1	40.5	33.6	14.4	−15.8 (0.1)
#14J	650	66.8	q	43.0	95.3	−1.2	−1.2	40.5	28.7	14.6	−16.0 (0.1)
#10J	750	0.04	q	47.8	97.5	−0.5	−0.4	41.8	40.2	16.6	−15.0 (0.3)
#10I	750	0.08	q	48.3	98.1	−0.5	−0.3	41.8	38.6	15.6	−14.6 (0.1)
#10H	750	0.17	q	48.7	96.7	−0.5	−0.4	41.8	38.6	15.7	−14.9 (0.1)
#10G	750	0.3	q	49.6	95.8	−0.5	−0.2	41.8	36.6	16.1	−14.7 (0.1)
#10K	750	0.7	q	47.0	98.1	−0.5	−0.2	41.8	36.1	15.5	−14.9 (0.1)
#10F	750	1.3	q	50.5	97.4	−0.5	−0.4	41.8	36.3	15.4	−15.2 (0.1)
#10L	750	2.7	q	46.1	98.0	−0.5	−0.5	41.8	33.9	14.6	−15.2 (0.1)
#5C	750	1.1	q	120.4	101.2	−0.4	−0.5	41.9	37.6	15[f]	−14.6 (0.1)

Table 5. (Continued)

Sample	T (°C)	Duration (days)	Tube[a]	μmoles CO_2 (initial)[b]	Yield (%)[b]	$\delta^{13}C_{PDB}$ (‰, initial)	$\delta^{13}C_{PDB}$ (‰, final)	$\delta^{18}O_{SMOW}$ (‰, initial)	$\delta^{18}O_{SMOW}$ (‰, final)	Tube length (cm)[c]	$\log_{10}(D)$ (cm^2/s)[d]
#5B	750	2.1	q	125.4	100.9	−0.4	−0.4	41.9	36.1	15[f]	−14.5 (0.1)
#5A	750	5.7	q	132.0	100.6	−0.4	−0.5	41.9	36.8	15[f]	−15.1 (0.1)
#5D	750	16.8	q	115.6	102.5	−0.4	−0.4	41.9	32.4	15[f]	−14.9 (0.1)
#5E	750	38.0	q	104.2	104.0	−0.4	−0.5	41.9	28.5	15[f]	−14.9 (0.1)
#14B	750	66.8	q	196.3	98.7	−1.2	−1.2	40.5	32.8	14.1	−15.2 (0.1)
#14C	750	152.8	q	189.8	97.6	−1.2	−1.3	40.5	31.1	15.3	−15.5 (0.1)
#14K	750	1.0	v	67.6	97.2	−1.2	−1.3	40.5	34.6	16.3	−14.3 (0.1)[e]
#14L	750	2.0	v	53.4	99.4	−1.2	−1.3	40.5	30.1	17.2	−13.9 (0.1)[e]
#14M	750	4.1	v	51.4	101.0	−1.2	−1.3	40.5	26.4	17.8	−13.3 (0.1)[e]
#14N	750	8.1	v	55.9	99.8	−1.2	−1.3	40.5	24.7	16.9	—[e]
#14H	750	30.8	v	203.1	99.1	−1.2	−1.2	40.5	27.7	15.6	−13.3 (0.1)[e]
#14I	750	66.8	v	209.5	99.2	−1.2	−1.3	40.5	23.1	16.4	—[e]
#10A	850	0.04	q	54.5	100.7	−0.5	−0.5	41.8	39.4	15.7	−14.5 (0.2)
#10B	850	0.08	q	53.7	99.8	−0.5	−0.4	41.8	38.5	16.4	−14.5 (0.1)
#10C	850	0.17	q	53.2	98.1	−0.5	−0.5	41.8	37.8	16.1	−14.6 (0.1)
#10D	850	0.3	q	51.4	99.2	−0.5	−0.5	41.8	37.2	15.3	−14.8 (0.1)
#10M	850	0.7	q	45.7	98.0	−0.5	−0.4	41.8	34.7	15.5	−14.7 (0.1)
#10E	850	1.3	q	51.4	98.4	−0.5	−0.3	41.8	34.1	15.1	−14.8 (0.1)
#10N	850	2.7	q	45.6	97.4	−0.5	−0.4	41.8	30.6	16.7	−14.9 (0.1)
#4L	850	10.2	q	41.8	97.4	−0.3	−0.4	41.8	24.5	15[f]	−14.7 (0.1)
#4K	850	20.8	q	37.0	93.8	−0.3	−0.6	41.8	23.8	15[f]	−15.1 (0.1)
#14A	850	66.8	q	205.9	98.2	−1.2	−1.1	40.5	30.1	15.1	−14.9 (0.1)

[a] v = Vycor tube; q = GE214 quartz glass tube.

[b] Measured number of μmoles of CO_2 loaded into the capsule at the start of the experiment and the measured yield of CO_2 extracted at the close of the experiment in percent of the initial, as loaded, value.

[c] Length of tube. Inside diameter of all tubes was 0.7 cm.

[d] Diffusion coefficient calculated as described in the text. Errors propagated assuming uncertainties in $\delta^{18}O_{SMOW}$ (final) of 0.3, in run duration of 0.01 days, in gas content of 1 μmole, in tube length of 1 cm, and in tube inner radius of 0.01 cm.

[e] The calculation of diffusion coefficients for experiments run in Vycor tubes assumed a fractionation factor equal to that determined for silica glass (*i.e.*, $\Delta \approx 3.25$ per mil). For one experiment (14N), the $\delta^{18}O_{SMOW}$ of the CO_2 at the end of the experiment was so close to the value expected at equilibrium with the Vycor tube that a meaningful D could not be calculated. In the case of experiment 14I, the final $\delta^{18}O_{SMOW}$ of the gas actually was within 3.25 per mil of the bulk Vycor tube, so no D was calculated in this case.

[f] Tube length not measured. Value of 15 cm assumed based on similarity to all other experiments.

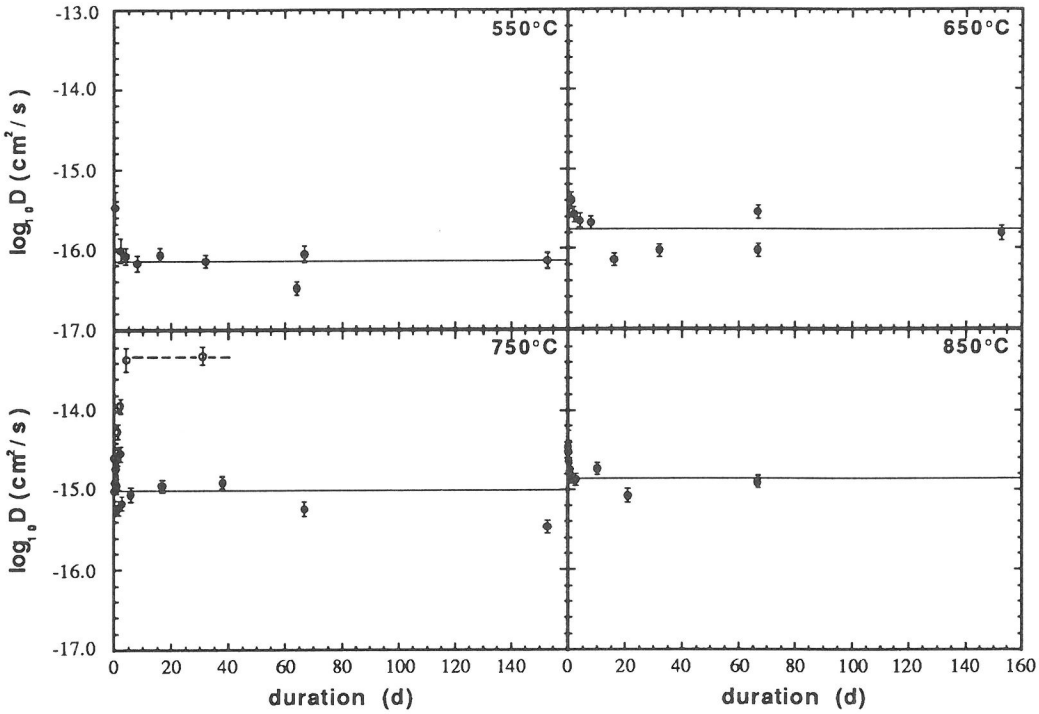

FIG. 4. Apparent self-diffusion coefficients for oxygen in silica (closed symbols) and Vycor (open symbols) glass as a function of run duration at temperatures of 550–850°C based on the experiments and calculations described in the text (data listed in Table 5). The solid horizontal lines show the average values for silica glass at each temperature based on runs of >0.5 days duration; runs of shorter duration were excluded to minimize the possible influence of surface exchange kinetics on the results. The dashed horizontal line at 750°C shows the approximate long duration value for Vycor glass.

increasing run duration, the final gas value increases slowly with time to a near constant value. Similar effects are also suggested by some of our diffusion experiments (discussed below) and were observed by LIU and EPSTEIN (1984) in hydrogen isotope exchange experiments between water vapor and kaolinite. Although we do not fully understand these phenomena, we have tried to avoid their influence by (1) basing our evaluations of equilibrium fractionation factors on the results of experiments run for long enough times that the results do not appear to be time dependent, thereby ensuring that substantial exchange occurred between the gas and oxygen deep within the silicate material (see discussion of diffusion experiments below); and (2) verifying our results using different starting materials and size fractions.

Kinetics of oxygen isotope exchange

The results of experiments in which only CO_2 gas was loaded into glass tubes are listed in Table 5. In order to extract quantitative information from these data, we assumed that the inner surface of the glass tube and the vapor were in local equilibrium (with fractionation factors as given in Table 4) and that simple interdiffusion of ^{18}O and ^{16}O occurs within the glass. The time dependence of the isotopic composition of the inner surface of the tube was then approximated by a polynomial. This led to a series solution to the diffusion equation, from which the self-diffusion coefficient for oxygen, D, was obtained for each experiment. D values are listed in Table 5 and shown in Fig. 4 as a function of run duration for each temperature.

Despite some scatter in the results, calculated D values for the silica glass tubes (which at 750°C are $\approx$2 orders of magnitude lower than calculated D values for the Vycor glass tubes) are essentially independent of time and of the amount of gas loaded into the tube, confirming the appropriateness of treating the exchange as a diffusive phenomenon. We do not have an explanation for the scatter in calculated D values at each temperature; it could reflect slightly different geometries for each sample (*i.e.*, the effects of the sealed ends of the tubes are

not considered in our treatment), the influence at short times and in the lower temperature experiments of surface exchange phenomena with different kinetics (possibly affected by partial equilibration of the inner surface of the tube with air during the preheating step), or irregularities in the inner surface of the tubes (*e.g.*, microcracks).

Figure 5 compares the temperature dependence of the self-diffusion coefficient for oxygen in silica glass based on our CO_2 exchange experiments with previous determinations, all of which were based on isotope exchange between glass and O_2 gas (HAUL and DÜMBGEN, 1962; SUCOV, 1963; WILLIAMS, 1965; MUEHLENBACHS and SCHAEFFER, 1977). Our results are consistent with the two most recent of these determinations; because these were based on high temperature experiments in which the effects of surface phenomena could definitively be ruled out, the similarity between their results and those from our long duration experiments conducted at lower temperature supports our conclusion that such phenomena play at most a minor role in our most lengthy experiments. In addition, WILLIAMS (1965) obtained similar results whether diffusion experiments were conducted on fine silica fibers or silica tubes; this is consistent with our finding that grain size and sample preparation techniques are not major factors in the results of long duration isotope exchange experiments.

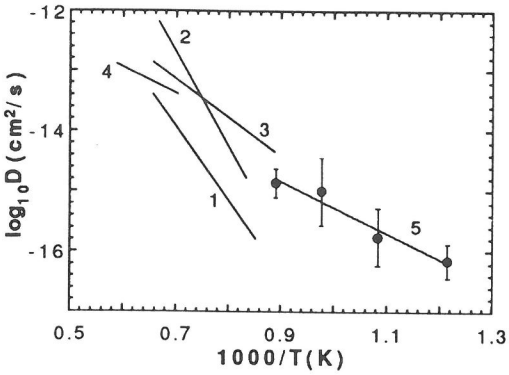

FIG. 5. Summary of data on the apparent oxygen self-diffusion coefficient in silica glass from this study and from the literature. Values from this study are averages of results of all runs of >0.5 days duration; error bars are $\pm 2\sigma$ based on the distribution of analyses used to calculate these average values. The line through our data is given by

$$\log_{10} D\ (cm^2/s) = -11.0(1.4) - 4.3(1.3) \times 10^3/T\ (K)$$

and corresponds to an activation energy of $\approx$20 kcal/mole. Numbers on lines refer to: 1—HAUL and DÜMBGEN (1962); 2—SUCOV (1963); 3—WILLIAMS (1965); 4—MUEHLENBACHS and SCHAEFFER (1977); 5—this work.

DISCUSSION

Evaluation of pitfalls

The most serious potential pitfall of our experiments is the possibility that the fractionation measured is between vapor and a surface layer rather than between vapor and bulk sample. Several observations and lines of reasoning suggest that this was not a major factor in most of our experiments.

Using our self-diffusion coefficients for oxygen in silica glass (Fig. 5), we calculate that for experiments lasting longer than about 18 days at 850°C, 6 weeks at 750°C, and 14 months at 550°C, the depth of penetration of oxygen exchange into silica glass is greater than about 1 μm. This is well into the bulk of the sample and indicates that the fractionation factors obtained from experiments of this duration are not likely to be influenced by surface effects. Experiments of at least these durations were conducted at each temperature, and inspection of the results (*e.g.*, Figs. 1 and 2) reveals that approximately constant $\delta^{18}O$ values for the gas, whether approached from heavier or lighter initial values, were achieved in runs of similar duration. In determining the "best" fractionation factors for each temperature, no runs in which calculated depths of penetration of exchange are less than 0.36 μm were used. For the GE214 experiments, the convergence of the results of experiments on several different size fractions to similar final $\delta^{18}O$ values at temperatures of $\geq$650°C also supports our conclusion that surface fractionations did not significantly influence our long duration results. Also consistent with this conclusion are the results of experiments covering a wide range of CO_2/silica glass ratios; in particular, indistinguishable results were obtained in 23–26 day experiments at 750°C whether the ratio of oxygen in glass wool to that in the vapor was 71 (run #4F) rather than the more typical value of about 300–500. We emphasize, however, as discussed above, that in short duration runs, there *is* evidence of the influence of surface phenomena in our experiments, including early rapid reaction, overshooting of the equilibrium values in short duration runs starting with gases with high initial $\delta^{18}O$ values (*e.g.*, experiments #22F and #22G at 650°C), and false convergences at anomalously light values (*e.g.*, experiments #7A and #7D at 650°C). Using our D values, we calculate depths of penetration of at most a few tenths of a micron under the conditions of the experiments that show such effects.

Note that even if exchange extends well into the sample, but the amount of vapor is too large or its initial isotopic composition is too far away from the value in equilibrium with the silicate, then the vapor may "see" a silicate in the exchanged layer

with an isotopic composition significantly different from the bulk silicate, leading to an incorrect fractionation factor if this effect were not taken into account. Although this effect is apparent in very few runs, in experiments on the coarsest size fractions of the GE214 material there is evidence of such incomplete convergence, with gas with an initial composition close to the equilibrium value more closely approaching the equilibrium value than gas with an initial value far from the equilibrium value (*e.g.*, compare #23P and #23T at 650°C). We minimized the potential impact of this problem on our results by choosing initial gas compositions close to the final value, by maximizing the silicate/vapor ratio, by decreasing grain size (in the GE214 experiments), by increasing run duration, or by some combination of these factors. The convergence of results from initially heavy and initially light CO_2 to final $\delta^{18}O$ values that are identical within error in long duration runs indicates that this effect of incomplete equilibration was not a problem in those runs most critical to us in evaluating fractionation factors. The lack of a dependence of the results on the ratio of the mass of CO_2 in an experiment to the mass of silica glass (*e.g.*, compare the results of #4F and #4H) also supports our contention that this effect was not significant in most of our experiments.

A second possible problem could be that interaction of the CO_2 vapor with the glass container may compete with exchange between vapor and the fine-grained sample, thus leading to spurious results. If this were a problem, we would expect the results of experiments conducted in Vycor tubes to be systematically heavier than those conducted in silica tubes, because the Vycor tubes are about 10 per mil heavier than the silica tubes (and heavier than the $\delta^{18}O$ gas values in equilibrium with the silica glass samples in all cases) and the apparent oxygen self-diffusion coefficient in Vycor is $\approx$2 orders of magnitude greater than in silica glass (Fig. 4). Except at 950°C, experiments conducted in Vycor and silica glass tubes yield indistinguishable results. It is especially significant that in GE214 experiments conducted in silica tubes, the tube and the powdered sample were both GE214 glass with the same $\delta^{18}O$ value; these experiments could not have been disturbed by equilibration with the tube, yet experiments in Vycor tubes and GE214 tubes yield indistinguishable results except at 950°C. In hindsight, the fact that the influence of the tubes is generally negligible is not surprising based on the D values determined for oxygen self-diffusion in silica glass. For example, in an experiment on one gram of silica glass wool with a thread diameter of 10 microns in which the diffusion front has penetrated $\leq$1 μm, the ratio of the number of oxygens exchanged in the glass wool to that exchanged in the enclosing glass tube would be about 50. At ratios this high, the effects of such interactions with the tube would generally be negligible. In extensions of the work reported here, we are using Pt tubes rather than glass to avoid entirely the possible influence of exchange with the container, but since this approach is significantly more expensive than using glass, we may return to our present methods for conditions at which interactions with glass containers can be shown to have negligible influence on the results.

Mechanism of isotopic exchange

The activation energy for self-diffusion given by our results (20 $\pm$ 3 kcal/mole) and the two most recent previous studies of oxygen isotope exchange between silica glass and O_2 vapor (20–29 kcal/mole; WILLIAMS, 1965; MUEHLENBACHS and SCHAEFFER, 1977) is low compared to that of oxygen self-diffusion in jadeite melt (assumed to be a nearly fully polymerized network of aluminosilicate tetrahedra as in silica glass) based on melt diffusion couples in which a vapor phase was not present ($\sim$60 kcal/mole; SHIMIZU and KUSHIRO, 1984) and compared to Si-O bond energies ($\sim$100 kcal/mole; DOREMUS, 1973). Our activation energy is, however, similar to those for O_2 permeation (22 kcal/mole; NORTON, 1961), O_2 diffusion (27–31 kcal/mole; BARRER, 1951; NORTON, 1961) and Ar diffusion (24–28 kcal/mole; PERKINS and BEGEAL, 1971; CARROLL and STOLPER, 1991) in silica glass. It is also similar to those for Ar (34 kcal/mole; CARROLL, 1991), molecular CO_2 (34 kcal/mole; BLANK *et al.*, 1991) and molecular H_2O (25 kcal/mole; ZHANG *et al.*, 1991a) in rhyolitic glass. This suggests to us that the exchange we observe is due to diffusion of molecular CO_2 into the glass, followed by exchange with the network of silicate tetrahedra, rather than actual self-diffusion of oxygen by exchange between oxygen sites of the network of silicate tetrahedra of which the glass is constructed. Based on similar reasoning, WILLIAMS (1965) and MUEHLENBACHS and SCHAEFFER (1977) concluded that O_2 mobility in the glass dominated the kinetics of isotope exchange between O_2 gas and fused silica.

ZHANG *et al.* (1991b) discuss in detail the relation between the apparent self-diffusion coefficient of oxygen and the diffusivity of a carrier in cases such as this in which the flux of oxygen is due to diffusion of the CO_2 carrier. One characteristic of such a diffusive process is that the apparent self-diffusion coefficient is equal to the product of the diffusivity of the carrier species and its concentration (provided

that there is only one carrier species; note that the activation energy of apparent self-diffusion based on exchange with a vapor will in general be even lower than that for diffusion of the carrier species, because it will include a contribution from the temperature dependence of the solubility of the carrier species). Thus, the diffusion coefficient for O_2 in silica glass based on permeation experiments is several orders of magnitude greater than the apparent self-diffusion coefficient based on isotopic exchange experiments (WILLIAMS, 1965), because the solubility of O_2 in silica glass under the conditions of the exchange experiments is very low. We therefore predict that if oxygen exchange is controlled by diffusion of CO_2 molecules into the glass as we have concluded, then the apparent self-diffusion coefficient of oxygen will vary approximately linearly with the fugacity of CO_2 in the experiments. From a practical standpoint, this suggests that enhancement of sluggish isotope exchange reactions could be achieved by conducting experiments at elevated fluid pressures, an effect observed by CHACKO *et al.* (1991) in exchange experiments between CO_2 and calcite at pressures up to 13 kbar. This effect was quantified by WILLIAMS (1965) who documented a proportionality between the self-diffusion coefficient of oxygen and pO_2 in exchange experiments between O_2 vapor and silica glass.

The fact that in silica glass the activation energies of diffusion of rare gases and neutral molecular species and the activation energy for self-diffusion of oxygen in exchange experiments with CO_2 gas are similar suggests, based on the discussion of ZHANG *et al.* (1991b), that the diffusion of CO_2 molecules is slow relative to the exchange reaction(s) between these molecules and oxygen sites in the glass. Otherwise, the apparent activation energy for self-diffusion should be higher than 20–30 kcal/mole due to a significant contribution from the activation energy for the exchange reaction, which we expect to be on the order of 100 kcal/mole since it requires the breaking of Si-O bonds. It may be that at sufficiently low temperatures, the exchange reaction becomes the rate limiting step as a consequence of its higher activation energy; this would be observable as an increase in slope of the Arrhenius plot for apparent oxygen self-diffusion. If oxygen exchange between CO_2 gas and silicate glass is rate limited by the diffusion of neutral CO_2 molecules, available results on diffusion of rare gases suggest that exchange may be even more rapid in more complex felsic glass compositions such as rhyolite, albite, and orthoclase, in which argon diffuses more rapidly at the temperatures of interest than it does in silica glass (CARROLL, 1991; CARROLL and STOLPER, 1991).

Temperature dependence of fractionation

The temperature dependence of isotopic fractionation factors between vapor and condensed phases can be complex (see O'NEIL, 1986), but the logarithm of the fractionation factor is expected to be approximately proportional to $1/T^2$ at high temperatures. Although our data can be described by such a relation at 650–950°C, our 550°C data points clearly deviate from such a linear trend and the overall trend of the data is slightly concave downwards toward the $10^6/T^2$ axis in Fig. 3.

Given values for the reduced partition function ratio for oxygen in CO_2 vapor (BOTTINGA, 1968; CHACKO *et al.*, 1991), our data can be used to calculate reduced partition function ratios for oxygen in silica glass. These calculated values are compared in Fig. 6 with the reduced partition function ratios for CO_2 vapor, quartz, and albite. Our data (which are basically linear in $1/T^2$) are well described by multiplying the reduced partition function ratio for crystalline quartz (CLAYTON *et al.*, 1989) by 1.035. The solid curves in Figs. 3 and 6 are based on such a reduced partition function ratio for silica glass.

In Fig. 7, we have replotted the data shown in Fig. 3 with $1/T$ as the abscissa. In this representation, the data are linear and the variation in $1000\ln(\alpha)$ calculated from the reduced partition function ratios is indistinguishable from a straight line. The slope of the tangent to a curve defining an exchange reaction plotted in these coordinates is equal to $-\Delta H^0/R$, where ΔH^0 is the standard state enthalpy

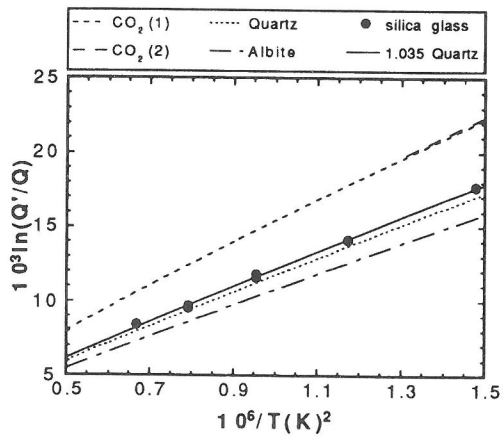

FIG. 6. Reduced partition function ratios versus $10^6/T(K)^2$. Curves for CO_2 are "CO_2 (1)" from CHACKO *et al.* (1991) and "CO_2 (2)" from BOTTINGA (1968). Curves for crystalline albite and quartz are from CLAYTON *et al.* (1989). Data points for silica glass (error bars are smaller than symbols) are from this study and were obtained by subtracting $1000\ln(\alpha)$ (Table 4) from the CO_2 reduced partition function ratio.

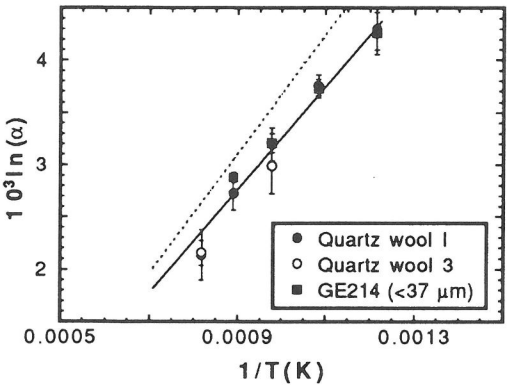

FIG. 7. Natural logarithm of the fractionation factor between CO_2 vapor and silica glass versus 1/T(K). Error bars as in Fig. 3. The solid curve (which is essentially a straight line in this temperature range) is calculated based on the reduced partition function ratios given for CO_2 in CHACKO *et al.* (1991) and 1.035 times the crystalline quartz-1 reduced partition function ratio given in CLAYTON *et al.* (1989). The dashed curve is the calculated CO_2-crystalline quartz fractionation factor based on these reduced partition function ratios.

change of the isotopic exchange reaction. The slope of the data shown in Fig. 7 corresponds to $\Delta H^0 \approx -10$ cal/mole.

Comparison to CO_2-quartz fractionation factors

Figure 3 shows, in addition to the CO_2-silica glass fractionation factor from our study, the calculated CO_2-quartz fractionation factor based on the reduced partition function ratio for crystalline quartz (CLAYTON *et al.*, 1989). The difference between the quartz and silica glass fractionations against CO_2 vapor suggests that silica glass is heavier than coexisting quartz by 0.3–0.6 per mil over the temperature range of this study. This difference is probably not resolvable at the present time given the uncertainties in our silicate and CO_2 gas analyses and those of CLAYTON *et al.* (1989) and CHACKO *et al.* (1991) on which the quartz-CO_2 fractionation is based. However, at the level of several tenths of a per mil, these results appear to confirm previous suggestions (GARLICK, 1966; MATSUHISA *et al.*, 1979) that oxygen isotope fractionations between crystalline and amorphous materials of the same composition and similar short-range structures are small.

Note that neither the quartz-CO_2 nor the silica glass-CO_2 fractionation factors are proportional to $1/T^2$ over the temperature range of these experiments (Fig. 3). However, the fractionation factor for oxygen isotopes between these two condensed phases does closely approximate this simple relation. This reflects the fact that the reduced partition function ratios for both of the condensed phases are roughly proportional to $1/T^2$ over this temperature range, but that of CO_2 is not (Fig. 6).

SUMMARY

(1) The fractionation of oxygen isotopes between CO_2 vapor and silica glass was determined at a total pressure of ~0.5 bars at temperatures of 550–950°C. The $^{18}O/^{16}O$ ratio of CO_2 vapor is higher than that of coexisting silica glass. The fractionation factor decreases from 1.0042 ± 0.0002 at 550°C to 1.0022 ± 0.0002 at 950°C.

(2) Ln(α) is linear with $1/T$ over the temperature range we investigated, corresponding to a standard state enthalpy change for the isotopic exchange reaction of approximately −10 cal/mole. The reduced partition function ratio for silica glass implied by our results is well described by 1.035 times that proposed for crystalline quartz by CLAYTON *et al.* (1989).

(3) Comparison of our results with data in the literature for quartz suggests that silica glass is enriched in ^{18}O relative to quartz with which it is in isotopic equilibrium by 0.3–0.6 per mil over the temperature range we have investigated. This small difference is probably not resolvable at present given the uncertainties but does confirm previous suggestions (GARLICK, 1966; MATSUHISA *et al.*, 1979) that oxygen isotope fractionations between crystalline and amorphous materials of the same composition and similar short-range structures are small. In contrast to the vapor-glass fractionation factor, the logarithm of the crystalline quartz-silica glass fractionation factor is expected to be roughly proportional to $1/T^2$ over the temperature range of this study.

(4) Experiments were conducted to determine the kinetics of oxygen isotopic exchange between CO_2 vapor and silica glass. The activation energy for the apparent self-diffusion of oxygen in silica glass is similar to those for diffusion of Ar and molecular CO_2, O_2, and H_2O in network glasses. This suggests that isotopic exchange in our experiments occurs by diffusion of CO_2 molecules into the glass followed by exchange with the oxygen atoms of the glass structure, and that the rate limiting step is the diffusion of the CO_2 molecules, not their reaction with the glass network. If so, oxygen isotopic exchange rates should be significantly enhanced in CO_2-glass experiments at elevated pressures.

(5) The success of our experiments suggests that the technique we used of equilibrating small amounts of vapor with large amounts of fine-grained solid, followed by analysis of the vapor, may be of

wide utility in determining isotopic fractionation factors, provided that, as we have done for silica glass, care is taken to distinguish bulk from surface fractionations and to demonstrate a close approach to equilibrium. This technique should be particularly useful for determining fractionation factors involving other framework glasses (*e.g.*, albite, orthoclase, etc.) that are known to have higher diffusivities of noble gases than does silica glass and for minerals with open structures into which water and carbon dioxide can readily diffuse.

Acknowledgements—We thank Ms. E. Dent for assistance with sample preparation and analysis, Dr. P. Dobson and Ms. J. Blank for assistance with some of the experiments, and Dr. S. Newman for help in sample characterization. We also thank Professor A. Matthews for invaluable advice and comments on this work, Professor Youxue Zhang for assistance in reducing the diffusion data, Professor R. Clayton and Ms. T. Mayeda for analyzing several of our starting materials, and Dr. J. Beckett, Professor J. R. O'Neil, and Professor H. P. Taylor for careful reviews. This work was supported by DOE Grant DE-FG03-85ER13445. Caltech Division of Geological and Planetary Sciences Contribution 5044.

REFERENCES

ANDERSON A. T., JR., CLAYTON R. N. and MAYEDA T. K. (1971) Oxygen isotope thermometry of mafic igneous rocks. *J. Geol.* **79,** 715–729.

BARRER R. M. (1951) *Diffusion In and Through Solids.* Cambridge University Press.

BLANK J. G., STOLPER E. M. and ZHANG Y. (1991) Diffusion of CO_2 in rhyolitic melt. *Eos* **72,** 312.

BOTTINGA Y. (1968) Calculation of fractionation factors for carbon and oxygen isotopic exchange in the system calcite-carbon dioxide-water. *J. Phys. Chem.* **72,** 800–808.

CARROLL M. R. (1991) Diffusion of Ar in rhyolite, orthoclase and albite composition glasses. *Earth Planet. Sci. Lett.* **103,** 156–168.

CARROLL M. R. and STOLPER E. (1991) Argon solubility and diffusion in silica glass: Implications for the solution behavior of molecular gases. *Geochim. Cosmochim. Acta* **55,** 211–225.

CHACKO T., MAYEDA T. K., CLAYTON R. N. and GOLDSMITH J. R. (1991) Oxygen and carbon isotope fractionations between CO_2 and calcite. *Geochim. Cosmochim. Acta* **55,** 2867–2882.

CHIBA H., CHACKO T., CLAYTON R. N. and GOLDSMITH J. R. (1989) Oxygen isotope fractionations involving diopside, forsterite, magnetite, and calcite: Application to geothermometry. *Geochim. Cosmochim. Acta* **53,** 2985–2995.

CLAYTON R. N., GOLDSMITH J. R. and MAYEDA T. K. (1989) Oxygen isotope fractionation in quartz, albite, anorthite, and calcite. *Geochim. Cosmochim. Acta* **53,** 725–733.

CONNOLLY C. and MUEHLENBACHS K. (1988) Contrasting oxygen diffusion in nepheline, diopside and other silicates and their relevance to isotopic systematics in meteorites. *Geochim. Cosmochim. Acta* **52,** 1585–1591.

DOREMUS R. H. (1973) *Glass Science.* J. Wiley & Sons.

GARLICK G. D. (1966) Oxygen isotope fractionation in igneous rocks. *Earth Planet. Sci. Lett.* **1,** 361–368.

HAUL R. and DÜMBGEN G. (1962) Untersuchung der Sauerstoffbeweglichkeit in Titandioxyd, Quarz und Quarzglas mit Hilfe des heterogenen Isotopenaustausches. *Z. Elektrochemie* **66,** 636–641.

LIU K. K. and EPSTEIN S. (1984) The hydrogen isotope fractionation between kaolinite and water. *Isotope Geosci.* **2,** 335–350.

MATSUHISA Y. (1979) Oxygen isotopic compositions of volcanic rocks from the East Japan island arcs and their bearing on petrogenesis. *J. Volcanol. Geotherm. Res.* **5,** 271–296.

MATSUHISA Y., GOLDSMITH J. R. and CLAYTON R. N. (1979) Oxygen isotope fractionation in the system quartz-albite-anorthite-water. *Geochim. Cosmochim. Acta* **43,** 1131–1140.

MUEHLENBACHS K. and KUSHIRO I. (1974) Oxygen isotope exchange and equilibrium of silicates with CO_2 or O_2. *Carnegie Inst. Wash. Yearb.* **73,** 232–236.

MUEHLENBACHS K. and SCHAEFFER H. A. (1977) Oxygen diffusion in vitreous silica—Utilization of natural oxygen abundances. *Canadian Mineral.* **15,** 179–184.

NORTON F. J. (1961) Permeation of gaseous oxygen through vitreous silica. *Nature* **191,** 701.

O'NEIL J. R. (1986) Theoretical and experimental aspects of isotopic fractionation. In *Stable Isotopes in High Temperature Geological Processes* (eds. J. H. VALLEY, H. P. TAYLOR, and J. R. O'NEIL); *Rev. Mineral.* **16,** pp. 1–40. Mineralogical Society of America.

O'NEIL J. R. and EPSTEIN S. (1966) Oxygen isotope fractionation in the system dolomite-calcite-carbon dioxide. *Science* **152,** 198–201.

PERKINS W. G. and BEGEAL D. R. (1971) Diffusion and permeation of He, Ne, Ar, Kr, and D_2 through silicon oxide thin films. *J. Chem. Phys.* **54,** 1683–1694.

PFEFFER R. and OHRING M. (1982) Network oxygen exchange during water diffusion in SiO_2. *J. Appl. Phys.* **52,** 777–784.

SHIMIZU N. and KUSHIRO I. (1984) Diffusivity of oxygen in jadeite and diopside melts at high pressures. *Geochim. Cosmochim. Acta* **48,** 1295–1303.

SUCOV E. W. (1963) Diffusion of oxygen in vitreous silica. *J. Amer. Ceram. Soc.* **46,** 14–20.

TAYLOR H. P., JR. (1968) The oxygen isotope geochemistry of igneous rocks. *Contrib. Mineral. Petrol.* **19,** 1–71.

WILLIAMS E. L. (1965) Diffusion of oxygen in fused silica. *J. Amer. Ceram. Soc.* **48,** 190–194.

ZHANG Y., STOLPER E. and WASSERBURG G. J. (1991a) Diffusion of water in rhyolitic glasses. *Geochim. Cosmochim. Acta* **55,** 441–456.

ZHANG Y., STOLPER E. and WASSERBURG G. J. (1991b) Diffusion of a multi-species component and its role in oxygen and water transport in silicates. *Earth Planet. Sci. Lett.* **103,** 228–240.